Multiple Resonance TADF Sensitizers Enable Green-to-Ultraviolet Photon Upconversion: Application in Photochemical Transformations

Yaxiong Wei, Ke Pan, Xiaosong Cao, Yuanming Li, Xiaoguo Zhou, and Chuluo Yang**

Dr. Y. Wei, K. Pan, Dr. X. Cao, Prof. C. Yang
Shenzhen Key Laboratory of Polymer Science and Technology, College of Materials Science and Engineering
Shenzhen University
Shenzhen 518060, China
E-mail: xcao@szu.edu.cn
clyang@szu.edu.cn

Y. Li, Prof. X. Zhou
Department of Chemical Physics
University of Science and Technology of China
Hefei, Anhui 230026, China

Keywords: Triplet-triplet annihilation upconversion, visible-to-UV upconversion, Multiple resonance, Photocatalysis.

Abstract

Efficient visible-to-ultraviolet (UV) triplet-triplet annihilation upconversion (TTA-UC) with large anti-Stokes shift is highly promising in solar-powered and indoor applications. Nonetheless, the excitation wavelength is confined to the blue region (< 450 nm) mainly due to large energy loss during triplet sensitization. Herein, a series of multiple resonance thermal activated delayed fluorescence (MR-TADF) compounds are constructed as pure organic sensitizers for the purpose of energy-loss reduction, which also feature intense absorbance at visible region, high intersystem crossing efficiencies, and long triplet lifetimes. By pairing the MR-TADF sensitizers with appropriate UV-emissive acceptors, green-to-UV TTA-UC systems were realized with anti-Stokes shift up to 1.05 eV, upconversion quantum yield up to 7.6% and threshold excitation intensity as low as 9.2 mW cm^{-2} in solution. Proof-of-concept demonstrations suggest the TTA-UC pairs could be applied as internal or external source of UV photons to trigger energy-demanding photopolymerization and photoligation reactions even under excitation of low-power-density green LED light, suggesting the broad utility of these molecular upconverters.

INTRODUCTION

Triplet-triplet annihilation upconversion (TTA-UC), or triplet fusion, is an anti-Stokes shifting technique that convert low-energy incident light under weak irradiation intensity to high-energy photon.[1-2] Comparing to other photon upconversion methods including two-photon absorption and rare-earth upconversion, TTA-UC enjoys low power density requirement and high upconversion quantum yield (Φ_{UC}),[3] and has attracted much attention in photovoltaics,[4-5] photocatalysis,[6-7] bioimaging,[8-9] organic light-emitting diodes,[10] circularly polarized luminescence,[11] and photoinduced drug release.[12] By pairwise selection of sensitizers and acceptors, TTA-UC system featuring adjustable excitation/emission wavelength have been demonstrated.[13-14] Notably, visible-to-UV upconversion is particularly valuable for enhancing the efficiency of photocatalytic systems including H_2 generation, CO_2 reduction and many organic reactions,[15-16] which always require highly energetic excited state for strong reduction or oxidation powers to induce challenging bond activation/formation reactions.[17]

Implementation of visible-to-UV TTA-UC with concurrent large anti-Stokes emission shift, high Φ_{UC}, and low power density threshold (I_{th}) is highly essential for solar-powered and indoor applications but remains elusive hitherto.[18] It is important to note that among all of reported visible-to-UV TTA-UC systems, the energy gains are less than 0.92 eV, restricting the excitation wavelengths in violet or blue region (**Figure S1** and **Table S1**). This limitation is mainly caused by the inherent energy loss during $S_1^* \rightarrow S_1$ vibrational relaxation (VR) and intersystem crossing (ISC) process of sensitizers.[19-20] As manifested in a Jablonski diagram in **Scheme 1a**, the sum of the

reorganization energy (λ_S^*) and the gap between singlet and triplet excited states (ΔE_{ST}) is always > 0.5 eV.[18, 21] To minimize energy loss for triplet sensitization, there have been recent advances by using direct S_0-T_1 absorption sensitizers, but low triplet energy (< 1.8 eV) and short triplet lifetime (~ 10^2 ns) of these complexes circumvent their use in visible-to-UV TTA-UC.[22-24] A more practical route is to adopt donor-acceptor (D-A) typed thermally activated delayed fluorescence (TADF) molecules owing to their energy degeneracy between excited states (ΔE_{ST} < 100 meV), which also allows efficient ISC courses from $S_1 \rightarrow T_1$ in the absence of noble metals.[25] For instance, several groups independently reported the use of carbazolyl dicyanobenzene based TADF molecules to sensitize *p*-terophenyl or pyrene derivatives, and achieved anti-Stokes shifts up to 0.83 eV under photoirradiation below 450 nm.[26-28] Nonetheless, the large structural flexibility of charge-transfer-featured S_1 state would result in substantial non-radiative energy loss, and cause weak absorption in the visible range to request large excitation threshold that was not even close to solar irradiance.[19]

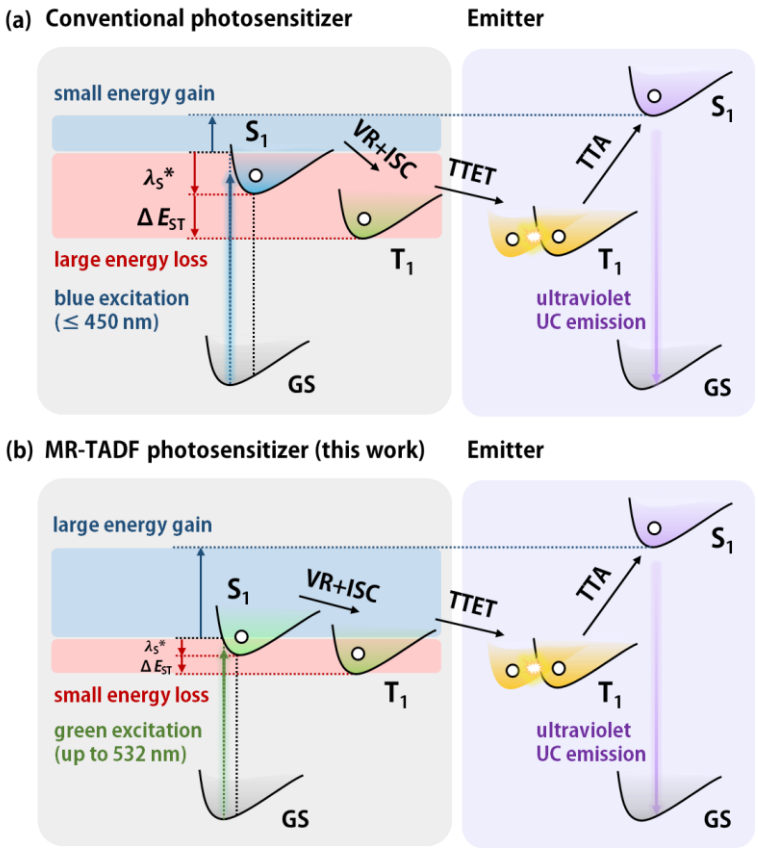

Scheme 1. The energy loss of (a) conventional photosensitizer and (b) MR-TADF photosensitizer with TTA-UC mechanism.

In this context, new sensitizers with satisfactory extinction coefficients (ε) in the long-wavelength range (*i.e.* > 500 nm) while maintaining high triplet energies (*i.e.* > 2.2 eV), high ISC efficiency (Φ_{ISC}), and long triplet lifetimes becomes an emergent request. It is also noted that development of metal-free organic triplet sensitizers is an ongoing pursue, considering the high expense and toxicity of precious- or rare-earth-metal-based complexes.[29-30] We hereby report for the first time highly efficient green-to-UV TTA-UC system operable with weak incident light by implementing multi-resonance TADF (MR-TADF) compounds as photosensitizing species, and demonstrate their potential application in photochemical reactions. The MR effect induced by *ortho*-

positioned electron-rich N-atom and electron-deficient B-atom in a rigid polycyclic aromatic hydrocarbon framework minimizes VR of S_1, and separates frontier molecular orbitals to promise small ΔE_{ST}.[31-32] Additionally, these compounds typically display much more intense absorption band caused by short-range charge-transfer, comparing to the D-A typed counterparts.[33] These features render MR-TADF compounds ideal candidates as triplet donor and broadens the choice of acceptors (**Scheme 1b**). To maximize anti-Stokes shift, energy loss during triplet-triplet energy transfer (TTET) is furtherly reduced by matching the MR-TADF sensitizers with appropriate UV-emissive acceptors to give small or even negative triplet energy gaps, eventually lead to unprecedentedly large energy gain of 1.05 eV among visible-to-UV TTA-UC systems.

RESULTS AND DISCUSSION

The advent of MR-TADF molecules has brought exciting opportunities for the fabrication of OLEDs with extraordinary efficiency and color purity,[25, 34] yet their potential as sensitizers remains underexplored. An important issue to be addressed is the insufficient Φ_{ISC} of MR-TADF compounds comparing to conventional (donor-acceptor typed) TADF fluorophore, as also reflected by smaller contribution of long-lived delayed components to the photoluminescence quantum yields (Φ_{PLS}).[35] This character is related to the pseudo spin-forbidden nature of $S_1 \rightarrow T_1$ transition with slightly enlarged energy differences (typically in the range of 100 meV ~ 200 meV).[33] To overcome the obstacle, we establish two MR-TADF compounds (BN-2Cz and BN-2Cz-*t*Bu, **Scheme 2a**) with twisted geometry as highly promising heavy-element-free

sensitizers (see Supporting Information for detailed synthetic procedures and characterizations). Importantly, the electronic donors (carbazole or 3,6-di-*tert*-butylcarbazole) orthogonally linked to the parent B,N-skeleton not only shifts the absorbance into green region but also guarantee high ISC efficiency.

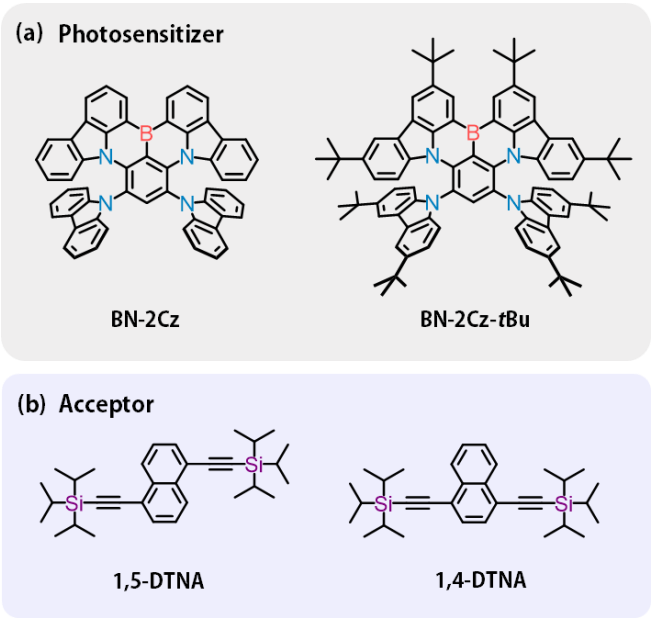

Scheme 2. The molecular structures of (a) sensitizers and (b) acceptors.

The UV-Vis absorption spectra, fluorescence and phosphorescence (recorded at 77 K) emission spectra were measured and shown in **Figure 1**. BN-2Cz displayed strong absorption band at 490 nm (ε = 2.37 × 10^5 M^{-1} cm^{-1}) in toluene, attributable to the multiple resonance charge transfer transition (**Figure 1a**). The intense mirroring fluorescence emission was located at 522 nm (Φ_{PL} = 70%), followed by the phosphorescence emission peaking at 554 nm (2.24 eV). Attaching *tert*-butyl (*t*-Bu) moieties to the 3,6-position of carbazole unit decreased the delocalization energy of electronic states and led to a moderate bathochromic shift of the absorption peak (504

nm, ε = 2.95 × 10^5 M^{-1} cm^{-1}). Meanwhile, the fluorescence and phosphorescence emission peaks were also shifted to 543 nm and 569 nm (2.20 eV), respectively, with Φ_{PL} as high as 84%. Accordingly, the total energy losses were estimated to be only 0.29 eV and 0.26 eV during triplet sensitization for BN-2Cz and BN-2Cz-*t*Bu (**Figure 1c**), respectively. These results also demonstrated that delicate manipulation of excited state energy levels would be possible *via* structural modification.[25]

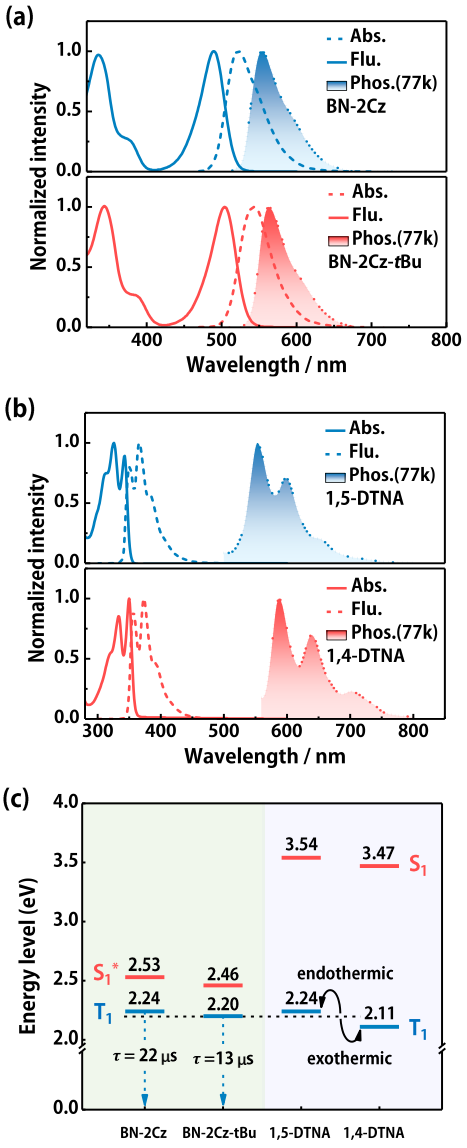

Figure 1. The normalized absorption, fluorescence and phosphorescence spectra of (a) (a) sensitizers and (b) acceptors; (c) the energy level of sensitizers and acceptors;

toluene as solvent.

Time-resolved transient photoluminescence (TRPL) measurements (λ_{ex} = 480 nm) unveiled distinct double-exponential decay profiles for both compounds in deoxygenated toluene solution, characteristic of TADF properties. The prompt fluorescence lifetimes (τ_ps) and delayed lifetimes (τ_ds) were determined to be 4.5 ns (24.9%) and 21.8 μs (75.1%) for BN-2Cz, 5.2 ns (40.5%) and 17.8 μs (59.5%) for BN-2Cz-*t*Bu, respectively (**Figure S9** and **S10**). The long-lived components for both compounds were strongly quenched in air-saturated solution, indicating the origination of delayed fluorescence from triplet states. Based on the Φ_{PL} values and transient PL decay characteristics, the ISC rates (k_{ISC}s) and Φ_{ISC}s were deduced to be 1.1 × 10^8 s^{-1} and 60% for BN-2Cz-*t*Bu, 1.7 × 10^8 s^{-1} and 75% for BN-2Cz, respectively, suggestive of efficient ISC process for triplet sensitization (**Table 1**). In stark contrast, the parent molecule BN without carbazole substituents exhibited similar ΔE_{ST} (0.15 eV) value but weak delayed fluorescence signal, with k_{ISC} = 1.1 × 10^7 s^{-1} and Φ_{ISC} = 5.8% (**Figure S8**). To uncover the inherent factors that governed these excited-state properties, we carried out TD-DFT calculations and predicted the spin-orbital coupling (SOC) matrix elements (ξ) between excited states for BN-2Cz-*t*Bu ($\xi_{S1\text{-}T1}$ = 0.112 cm^{-1}, $\xi_{S1\text{-}T2}$ = 0.653 cm^{-1}), BN-2Cz ($\xi_{S1\text{-}T1}$ = 0.116 cm^{-1}, $\xi_{S1\text{-}T2}$ = 0.802 cm^{-1}, **Table S5**) and BN ($\xi_{S1\text{-}T1}$ = 0.054 cm^{-1}, $\xi_{S1\text{-}T2}$ = 0.131 cm^{-1}). Since $\Delta E_{S1\text{-}T2}$s were small enough in all cases (<0.16 eV, **Table S6**), these results hinted the transition between S_1/T_2 could be a more efficient ISC pathway comparing to S_1/T_1 with nearly identical orbital parentage, in line with El-

Sayed rules.[36-37] Importantly, the introduction of auxiliary donating groups to form a twisted D-A geometry was the key to induce much larger orbital difference between S_1 and T_2 in BN-2Cz-*t*Bu and BN-2Cz (**Figure S27**),[38] which consequentially facilitated the spin flip transition and made them more suitable sensitizer candidates.

Table 1. The photophysical parameters of photosensitizers and acceptors.

Compound	$\lambda_{Abs.}$ [a]	$\lambda_{Em.}$ [b]	$\lambda_{Phos.}$ [c]	Φ_{PL} [d]	Φ_{ISC} [e]	k_q [f]	Φ_{UC}, [g]
BN-2Cz	490 (2.37)	522	554	70	75	1.34 (0.95)	7.6 (6.4)
BN-2Cz-tBu	504 (2.95)	543	563	84	60	0.25 (0.08)	6.0 (5.0)
1,5-DTNA	326 (1.95) 343 (1.74)	350/366	554/599	73	-	-	-
1,4-DTNA	333 (2.85) 350 (3.34)	357/373	588/638	81	-	-	-

[a]The maximum absorption peaks, nm (molar extinction coefficient, 10^5 M^{-1} cm^{-1}); [b]The emission peaks, nm; [c]the phosphorescence emission peaks, nm (the triplet energy); [d]absolute fluorescence quantum yield in Ar, %; [e]the ISC efficiency, %; [f]the biomolecular quench rate constant with 1,4-DTNA as acceptor (1,5-DTNA as acceptor), 10^9 M^{-1} s^{-1}; [g]The Φ_{UC} with 1,4-DTNA as acceptor (1,5-DTNA as acceptor), %.

The tiny Stokes shifts and high triplet energy levels (2.20 eV ~ 2.24 eV) of BN-2Cz and BN-2Cz-*t*Bu allowed them to pair with UV-emissive triplet acceptors. By referring to a recent report by Kimizuka et al.,[18] 1,4-bis((triisopropylsilyl)ethynyl)naphthalene (1,4-DTNA, **Scheme 2b**) would be a suitable acceptor due to its appropriate triplet energy (T_1 = 2.11 eV) and high statistical probability to generate singlet excited state (f = 32%). It is also anticipated that chemical

structure modification of ethynyl naphthalene derivatives would allow simultaneous manipulation of both singlet and triplet excited states, thus minimizing enthalpic energy loss in TTET and maximizing the anti-Stokes shift value. Based on computational results for a series of isomers (**Figure S30**), a new acceptor (1,5-DTNA) was also constructed with a smaller π-conjugated structure and slightly higher triplet energy. Correspondingly, toluene solution of 1,5-DTNA (0.01 mM) displayed hypsochromic shifted 0-0 absorption peak at 343 nm (ε = 1.74 × 10^5 M^{-1} cm^{-1}) comparing to that of 1,4-DTNA (350 nm, ε = 3.34 × 10^5 M^{-1} cm^{-1}) (**Figure 1b**, **Table 1**). Following a similar trend, the 0-0 vibronic fluorescence and phosphorescence peaks were located at 350 nm, 554 nm (2.24 eV) for 1,5-DTNA, and 357 nm, 588 nm (2.11 eV) for 1,4-DTNA. The Φ_{PL} of 1,5-DTNA (73.3% in Ar) was only slightly lower than that of 1,4-DTNA (80.5% in Ar). Based on the energy relationships (Figure 1c), the sensitizer/acceptor pairs are separated into two categories: BN-2Cz/1,4-DTNA, BN-2Cz/1,5-DTNA and BN-2Cz-*t*Bu/1,4-DTNA as exothermic/isoenergetic systems, and BN-2Cz-*t*Bu/1,5-DTNA as endothermic systems. Though energy transfer process in the latter combination is thermodynamically unfavorable, the energy barrier is still sufficiently small (0.04 eV) to allow thermally activated TTET.[39] According to precedent reports,[39] long triplet lifetime of the sensitizer is also beneficial to suppress the deleterious reverse triplet energy transfer (RTET) process, which is a primary cause of low efficiency in endothermic systems. It is hence expected pairing sensitizer and acceptor with negative energy difference (ΔE_T) would be viable in our study to enlarge energy gain without significantly deteriorating the TTA-UC performance.[39]

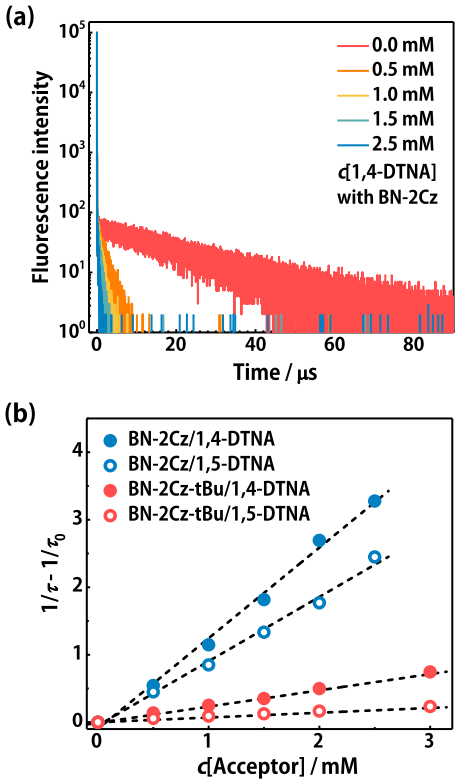

Figure 2. (a) Variation of delayed fluorescence lifetime of BN-2Cz with changes in the concentration of the acceptor 1,4-DTNA; (b) the bimolecular quenching rate generated from the delayed fluorescence lifetime quenching curves; *c*[photosensitizer] = 0.01 mM, λ_{ex} = 480 nm, toluene as solvent.

The TTET process was subsequently investigated between sensitizers and acceptors (**Figure 2a** and **S10 - S12**). For instance, the delayed fluorescence was gradually quenched upon titration of the BN-2Cz solution with 1,4-DTNA, indicating the occurrence of effective TTET from the sensitizer to the acceptor (**Figure 2a**).[40] The observed bimolecular quenching rate constant (k_{TTET}) values derived from the Stern-Volmer plots (**Figure 2b**) were determined to be 1.34×10^9 M^{-1} s^{-1} for BN-2Cz/1,4-DTNA and 0.95×10^9 M^{-1} s^{-1} for BN-2Cz/1,5-DTNA, and allowed the use of relatively

low concentration of acceptors ([sensitizer] = 0.01 mM, [acceptor] = 1 mM) to reach satisfactory TTET efficiency (Φ_{TTETs} > 95%, **Table S2**). By replacing the sensitizer with BN-2Cz-*t*Bu, the collision energy transfer process was mitigated according to drastically lowered k_{TTET} of 0.25 × 10^9 M^{-1} s^{-1} for BN-2Cz-*t*Bu/1,4-DTNA. This phenomenon was associated with shielded spin-density surface of T_1 by the insulating *t*-Bu groups that clearly lowered the Dexter electron exchange probability between energy transfer pairs (**Figure S27**).[41] Due to the endothermic nature, BN-2Cz-*t*Bu/1,5-DTNA presented even smaller k_{TTET} of 0.08 × 10^9 M^{-1} s^{-1}. To compensate the retarded TTET when using BN-2Cz-*t*Bu as the sensitizer, we optimized [acceptor] to 5 mM in the following TTA-UC measurements to attain relatively high Φ_{TTETs} value of 94% for BN-2Cz-*t*Bu/1,4-DTNA and 82% for BN-2Cz-*t*Bu/1,5-DTNA (**Table S3**). Notably, increasing [acceptor] is also vital for suppression the notorious RTET process and provide an entropic driving force in endothermic systems. For BN-2Cz-*t*Bu/1,5-DTNA (ΔE_T = -0.04 eV) specifically, the effect of RTET on TTA-UC performance could be neglected with optimized [acceptor] based on the following relationship: k_{RTET} × [sensitizer] = 0.32 × 10^4 s^{-1} << k_{TTET} × [acceptor] = 0.35×10^6 s^{-1}, where the k_{RTET} was estimated to be 0.32 × 10^9 M^{-1} s^{-1} from the equation $k_{RTET} = k_{TTET} \times exp(-\frac{\Delta E_T}{k_B T})$.[42]

TTA-UC investigations employing the MR-TADF sensitizers and ethynyl naphthalene-based acceptors were subsequently conducted under 517 nm photoexcitation. Intense fluorescence in the range of 330 nm - 440 nm that overlapped with the emission of the acceptors could be detected in a deaerated toluene solution of BN-2Cz (0.01 mM) and DTNA (**Figure 3a**), accompanying with significantly

prolonged fluorescence lifetimes (τ_{DF} = 287 μs for BN-2Cz/1,4-DTNA system, 134 μs for BN-2Cz/1,5-DTNA system), clearly manifesting the long-lived triplet-mediated mechanism (**Figure S31**).[18] Likewise, strong delayed emission in UV region could also be obtained by using BN-2Cz-*t*Bu (**Figure 3a** and **S32**). In all these systems, remarkable anti-Stokes shifts ranging from 0.91 eV (375 nm ← 517 nm) for 1,4-DTNA as acceptor to 0.98 eV (367 nm ← 517 nm) for 1,5-DTNA as acceptor were recorded, deduced by the energy difference between excitation wavelength and the maximum UC emission peaks. Noteworthily, since the red-shifted absorption band of BN-2Cz-*t*Bu extended down to over 540 nm, photoexcitation of the BN-2Cz-*t*Bu/1,5-DTNA system with 532 nm laser was also feasible to produce intense UC emission (**Figure S24** and **S25**), offering a remarkable anti-Stokes shift up to 1.05 eV (367 nm ← 532 nm). To the best of our knowledge, this is the first report to realize efficient low-power green-to-UV TTA-UC, with unprecedented anti-Stokes shift values for visible-to-UV upconversion systems (**Table S1** and **Figure S1**).

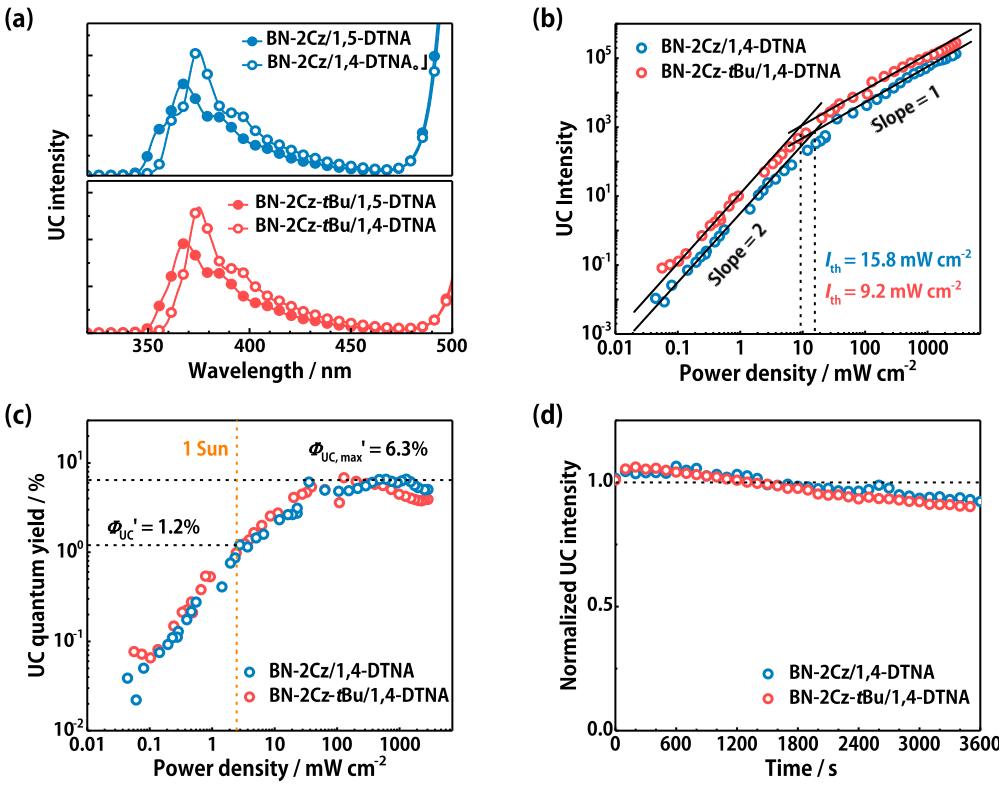

Figure 3. (a) Upconverted fluorescence emission spectra of photosensitizers and acceptors; (b) double logarithmic plot of the upconverted fluorescence intensity as a function of excitation power density in TTA-UC; (c) double logarithmic plot of Φ_{UC}'s as a function of excitation power density, Red line indicates the intensity of sunlight (2.6 mW cm^{-2}, **Figure S19**); (d) upconversion intensity at 370 nm at I_{ex} = 160 mW cm^{-2} for 1 hour; toluene as solvent.

The Φ_{UC}' values (with the theoretical limit standardized to be 100%) deduced by the relative quantum yield method of BN-2Cz (0.01 mM) were up to 7.6% and 6.4% when pairing with 1,4-DTNA and 1,5-DTNA, respectively, under 517 nm excitation (**Figure S20 – S24**).[43] The higher values acquired by using 1,4-DTNA were in line with the acceptor's superior absolute fluorescence quantum yield. Switching the sensitizer to BN-2Cz-*t*Bu (0.01 mM) led to only slightly decreased Φ_{UC}'s (6.0% for 1,4-DTNA as

acceptor, 5.0% for 1,5-DTNA as acceptor) because of the inferior ISC rate and TTET efficiencies. It would hence be reasonable to conclude that the RTET process in the non-exothermic system was successfully suppressed. Delightfully, the Φ_{UC}' values of BN-2Cz-*t*Bu-based systems under 532 nm excitation could still approach 6.1% with 1,4-DTNA as acceptor and 4.0% with 1,5-DTNA (**Figure S25** and **S26**). These results are among the best records for pure-organic visible-to-UV upconversion systems (**Figure S1** and **Table S1**). It is envisaged that the efficiencies could be further promoted by structural optimization of the MR-TADF sensitizer to enhance the ISC efficiency (*i.e.* introducing heavy elements such as Ge, S, Se).

The threshold excitation power density I_{th}, where a quadratic-to-linear dependence of upconversion intensity on excitation power densities occurs, is another key indicator to evaluate TTA-UC systems besides conversion wavelengths and efficiencies.[44-46] This parameter directly associates with the sensitizer absorbance and TTET efficiency.[47] In order to reduce I_{th} values, the concentration of sensitizer was set to 0.1 mM. As illustrated in **Figure 3b**, the BN-2Cz/1,4-DTNA system showed a slope change from 2 to 1 in the log-log plot of UC emission against the laser power density, and the I_{th} was determined to be as low as 15.8 mW cm^{-2}. Due to a larger molar extinction coefficient of BN-2Cz-*t*Bu at 517 nm, I_{th} was further reduced to 9.2 mW cm^{-2} in BN-2Cz-*t*Bu/1,4-DTNA, a value 88% lower than that of the reported vis-to-UV TTA-UC system adopting conventional TADF sensitizer (75 mW cm^{-2}).[48] According to **Figure 3c**, the Φ_{UC}' values were maintained as high as 6.8% for these samples even at increased concentration of sensitizer, indicating the undesirable photon reabsorption and singlet

Förster energy transfer were insignificant. Remarkably, since the obtained I_{th}s were quite close to the solar irradiance (AM 1.5) of 2.6 mW cm^{-2} for BN-2Cz and 3.3 mW cm^{-2} for BN-2Cz-*t*Bu (0.1 mM, path length = 1 mm, **Figure S19**), the Φ_{UC}' values could still reach 1.2% at the solar irradiance. For 1,5-DTNA as acceptor, the I_{th} values were moderately raised to 41.8 mW cm^{-2} for BN-2Cz and 29.2 mW cm^{-2} for BN-2Cz-*t*Bu (**Figure S18**).

As an important aspect for practical applications, the inherent photostability of the upconversion systems was tested (**Figure 3d** and **Figure S26**) by monitoring the emission intensity at 370 nm under 517 nm photoexcitation with a power density of 160 mW cm^{-2}. After 1 hour irradiation, the upconversion intensity of most systems remained above 90% of their initial value, *i.e.*, 94% for BN-2Cz/1,4-DTNA, 92% for BN-2Cz/1,5-DTNA (**Figure 3d**), and 90% for BN-2Cz-*t*Bu/1,4-DTNA (**Figure S26**). Comparatively, a 24% decay of intensity occurred in BN-2Cz-*t*Bu/1,5-DTNA mixture (**Figure S26**), ascribable to the long-lived triplet excited state of BN-2Cz-*t*Bu and the lower TTET efficiency that maybe susceptible to undesirable side reactions. These results reflected high Φ_{TTET} may be beneficial to the photostability.

Stimulated by the high upconversion efficiency, low threshold excitation intensity and large anti-Stokes shift of our green-to-UV upconversion systems, photocatalytic reactions using green light were subsequently demonstrated. Albeit near-infrared to visible TTA-UC has been applied to drive several organic reactions,[6, 49-50] majority of valuable photochemical transformations rely on UV irradiation due to insufficient energy input from single visible photon.[51-52] Meanwhile, existing reports about visible-

to-UV TTA-UC for photocatalytic reaction all use intense blue light as excitation source (*e.g.* mercury lamps), which undoubtedly limit the application scope.

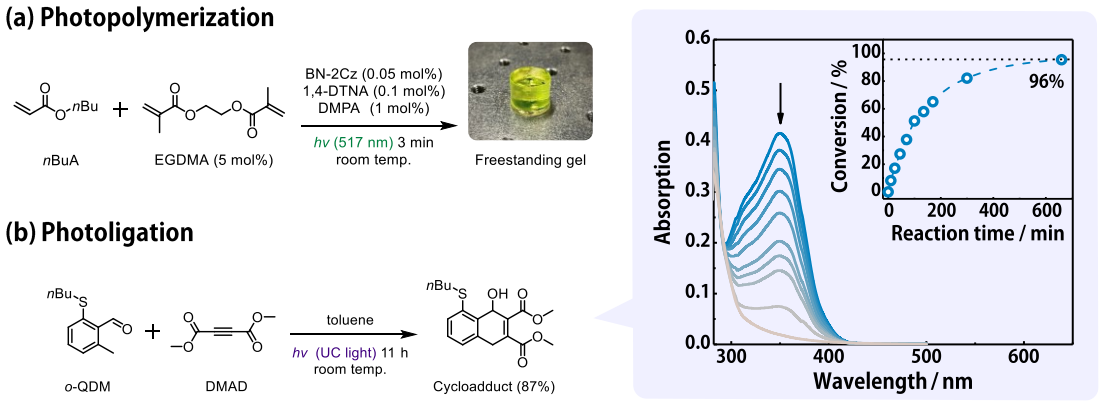

Figure 4. (a) Photoinitiated radical polymerization. *n*BuA/EGDMA = 90/10 (v/v), *c*[BN-2Cz] = 0.1 mM, *c*[1,4-DTNA] = 1 mM, λ_{ex} = 517 nm, I_{ex} = 80 mW cm^{-2}, toluene as solvent; (b) photoligation reactions and the change of absorption spectra of *o*-QDM + DMAD with photoirradiation time, the inset is the reaction conversion of A1, *c*[*o*-QDM] = 5 mM, *c*[DMAD] = 6.25 mM, *c*[BN-2Cz] = 0.05 mM, *c*[1,4-DTNA] = 1 mM, λ_{ex} = 517 nm, I_{ex} = 300 mW (The size of laser spot is 5mm), toluene as solvent.

Photo-activated free radical polymerization has been a powerful synthetic tool applicable in dental cares, non-toxic packaging, and 3D-printing due to its versatility and biocompatibility.[53-55] While typical photoinitiators only absorb short-wavelength photons (mostly UV), UV light sources are eco-unfriendly with the formation of ozones, and also present severe thermal effect and shallow penetration depth.[56] As a proof of concept, we integrated BN-2Cz/1,4-DTNA with the commercially available UV-absorbing 2,2-dimethoxy-2-phenylacetophenone (DMPA) as a green light

photoinitiating system, which was applied for the polymerization of *n*-butylacrylate (*n*BA, as monomer) and ethylene dimethacrylate (EGDMA, as cross-linker).[51] DMPA has absorption band overlapped with the TTA-UC emission greatly (**Figure S36**), and undergo the Norrish type I α-cleavage to produce free-radical species upon photon absorption. In a 2-mL-scale reaction, the mixture was rapidly transformed into a transparent freestanding gel upon irradiation with 517 nm laser (80 mW cm^{-2}, 2 min), while no gelation occurred in control experiments in the absence of BN-2Cz or 1,4-DNTA after 30 min (**Figure 4a** and **S41**), confirming the necessity of TTA-UC. Benefited from efficient UV photon production even under low excitation intensity, altering the light source to 517 nm LED (6.3 mW cm^{-2}, 20 min, **Figure S34** and **S38**) yielded a gel at the same reaction scale. The increased penetrability of green light through the reaction media also enabled photocuring in a scale-up reaction (35 mL, curing depth = 4.5 cm) to produce homogeneous gel upon green LED exposure for 2 hours (**Figure S42**). The above demonstrations clearly manifested the good sensitivity of TTA-UC pair to weak incident light and its sufficient chemical stability to survive highly reactive radical species.

Instead of serving as internal lamps to trigger photoreactions, the TTA-UC pair could be also applied as external UV source by segregating the upconversion system and reaction system into two different vessels. This strategy is particularly useful under certain circumstances such as thermodynamically challenging photoreactions, and may also avoid unwanted absorption/emission interference in product detection, simplify the workup procedure in photo-isomerization, or photo-click reactions.[57] To establish this

concept, the UV-induced ligation of *o*-quinodimethanes, a non-catalyzed Diels-Alder reaction recently reported by Goldmann *et al.* (**Figure 4b**),[52] was selected as model reaction. As most of the non-catalyzed photoligations are operable only by UV irradiation, it is hence of great significance to extend the excitation to long-wavelength region by leveraging TTA-UC. Specifically, by immersing the inner vial containing BN-2Cz/1,4-DTNA in the solution mixture of two substrates *o*-methylbenzaldehydes (*o*-QDM, photocaged diene) and dimethyl acetylenedicarboxylate (DMAD, dienophile) (**Figure S33**), efficient reaction took place when excited with a 517 nm laser beam (300 mW cm^{-2}). As shown in **Figure 4b**, the n-π^* band absorption intensity of *o*-QDM at 350 nm gradually decreased with increasing photoirradiation time, clearly suggesting the depletion of *o*-QDM (**Figure S35**).[52] The conversion of *o*-QDM reached 96% after photoirradiation of 11 h (Figure 6b inset) to provide the Diels-Alder adduct and the 4π-electrocyclization side product in a similar ratio (90:10) with the preceding result based on ^{1}H NMR measurement.[52] The turnover number (TON) for the reaction mixture was 240 regarding to the sensitizer. Comparatively, less than 5% *o*-QDM was converted in the absence of inner vial (control) due to energy mismatch between the excitation wavelength (517 nm) and absorption of *o*-QDM (< 420 nm) (**Figure S35** and **S37**), indicating the photoligation was enabled *via* reabsorption of TTA-UC emission by the substrate (**Figure S36**). In addition, under green LED (6.3 mW cm^{-2}) irradiance, a moderate conversion of *o*-QDM (11%) was still noticed with 18 h photoirradiation, while negligible conversion (<1%) took place in the control experiment (**Figure S39**). The long-term stability and high efficiency reflected herein promised the potential of

using these TTA-UC pairs in other challenging photochemical transformations under mild visible-light excitation.

CONCLUSIONS

To sum up, a series of pure organic MR-TADF sensitizers featuring unique electronic structures have been developed and applied to construct green-to-UV TTA-UC systems with energetically suitable acceptors. Due to small vibrational relaxation and tiny ΔE_{ST} of the MR-TADF compounds, the energy loss is minimized during triplet sensitization process, eventually lead to unprecedented energy gain up to 1.05 eV in visible-to-UV region. In addition, benefited by the large molar extinction coefficient, high ISC yield and long triplet lifetime of the sensitizers, the TTA-UC systems exhibit high Φ_{UC}' (~ 7.6%) with low I_{th} values (~ 9.2 mW cm^{-2}) close to the solar irradiance. The TTA-UC pairs could be utilized as stable internal or external phototransducer to activate UV-dependent polymerization and catalyst-free ligation under green light irradiation with weak intensity. Considering the structural versatility of MR-TADF compounds, there remains plenty of space to improve the comprehensive performance of visible-to-UV molecular upconverters with furtherly enlarged anti-Stokes shift, which would hold great promise for a variety of practical applications including photovoltaics and photocatalysis.

ASSOCIATED CONTENT

Supporting information

The detail synthesis procedures and structural characterization data of the triplet sensitizers and acceptors, description of the equipment and methods, detail to UC quantum yield measurement, detail to the photochemical experiment studies are available in the Supporting Information. The UC samples in toluene is prepared and sealed in glove box (O_2 < 10 ppm). And a semiconductor laser 517 nm or 532 nm was used for the UC measurements. The anti-Stokes shift is determined by the different energy value of the maximum UC emission peaks and the excitation wavelength.

AUTHOR INFORMATION

NOTES

The authors declare no competing financial interest.

ACKNOWLEDGMENTS

We gratefully acknowledge the financial support from the Natural Science Foundation of China (Grant Nos. 51903159 and 91833304), and the Shenzhen Science and Technology Program (KQTD20170330110107046, JCYJ20190808151209557). We thank the Instrumental Analysis Center of Shenzhen University for analytical support.

Reference

(1) Gray, V.; Dzebo, D.; Abrahamsson, M.; Albinsson, B.; Moth-Poulsen, K., Triplet-Triplet Annihilation Photon-Upconversion: Towards Solar Energy Applications. *Phys. Chem. Chem.*

Phys. **2014**, *16*, 10345-10352.

(2) Zhao, J.; Ji, S.; Guo, H., Triplet–Triplet Annihilation Based Upconversion: From Triplet Sensitizers and Triplet Acceptors to Upconversion Quantum Yields. *RSC Adv.* **2011**, *1*, 937-950.

(3) Joarder, B.; Yanai, N.; Kimizuka, N., Solid-State Photon Upconversion Materials: Structural Integrity and Triplet-Singlet Dual Energy Migration. *J. Phys. Chem. Lett.* **2018**, *9*, 4613-4624.

(4) Cheng, Y. Y.; Fückel, B.; MacQueen, R. W.; Khoury, T.; Clady, R. G. C. R.; Schulze, T. F.; Ekins-Daukes, N. J.; Crossley, M. J.; Stannowski, B.; Lips, K.; Schmidt, T. W. Improving the light-harvesting of amorphous silicon solar cells with photochemical upconversion. *Energy Environ. Sci.* **2012,** *5*, 6953-6959

(5) Hill, S. P.; Hanson, K., Harnessing Molecular Photon Upconversion in a Solar Cell at Sub-Solar Irradiance: Role of the Redox Mediator. *J. Am. Chem. Soc.* **2017**, *139*, 10988-10991.

(6) Bilger, J. B.; Kerzig, C.; Larsen, C. B.; Wenger, O. S., A Photorobust Mo(0) Complex Mimicking [Os(2,2'-Bipyridine)3](2+) and Its Application in Red-to-Blue Upconversion. *J. Am. Chem. Soc.* **2021**, *143*, 1651-1663.

(7) Pfund, B.; Steffen, D. M.; Schreier, M. R.; Bertrams, M. S.; Ye, C.; Borjesson, K.; Wenger, O. S.; Kerzig, C., Uv Light Generation and Challenging Photoreactions Enabled by Upconversion in Water. *J. Am. Chem. Soc.* **2020**, *142*, 10468-10476.

(8) Kimizuka, N.; Sasaki, Y.; Oshikawa, M.; Bharmoria, P.; Kouno, H.; Hayashi-Takagi, A.; Sato, M.; Ajioka, I.; Yanai, N., Near-Infrared Optogenetic Genome Engineering Based on Photon Upconversion Hydrogels. *Angew. Chem. Int. Ed.* **2019**, *58*, 17827-17833.

(9) Yang, Z.-S.; Ning, Y.; Yin, H.-Y.; Zhang, J.-L., Lutetium(Iii) Porphyrinoids as Effective Triplet Photosensitizers for Photon Upconversion Based on Triplet–Triplet Annihilation (Tta). *Inorg. Chem. Front.* **2018**, *5*, 2291-2299.

(10) Graf von Reventlow, L.; Bremer, M.; Ebenhoch, B.; Gerken, M.; Schmidt, T. W.; Colsmann, A., An Add-on Organic Green-to-Blue Photon-Upconversion Layer for Organic Light Emitting Diodes. *J. Mater. Chem. C* **2018**, *6*, 3845-3848.

(11) Han, J.; Duan, P.; Li, X.; Liu, M. H., Amplification of Circularly Polarized Luminescence through Triplet-Triplet Annihilation-Based Photon Upconversion. *J. Am. Chem. Soc.* **2017**, *139*, 9783-9786.

(12) Huang, L., Zhao, Y., Zhang, H., Huang, K., Yang, J., & Han, G, Expanding Anti-Stokes Shifting in Triplet-Triplet Annihilation Upconversion for in Vivo Anticancer Prodrug Activation. *Angew. Chem. Int. Ed.* **2017**, *56*, 14400-14404.

(13) Wei, Y.; Zheng, M.; Chen, L.; Zhou, X.; Liu, S., Near-Infrared to Violet Triplet-Triplet Annihilation Fluorescence Upconversion of Os(Ii) Complexes by Strong Spin-Forbidden Transition. *Dalton Trans.* **2019**, *48*, 11763-11771.

(14) Haruki, R.; Sasaki, Y.; Masutani, K.; Yanai, N.; Kimizuka, N., Leaping across the Visible Range: Near-Infrared-to-Violet Photon Upconversion Employing a Silyl-Substituted Anthracene. *Chem. Commun.* **2020**, *56*, 7017-7020.

(15) Majek, M.; Faltermeier, U.; Dick, B.; Perez-Ruiz, R.; Jacobi von Wangelin, A., Application of Visible-to-Uv Photon Upconversion to Photoredox Catalysis: The Activation of Aryl Bromides. *Chem–Eur. J.* **2015**, *21*, 15496-501.

(16) Khnayzer, R. S.; Blumhoff, J.; Harrington, J. A.; Haefele, A.; Deng, F.; Castellano, F. N., Upconversion-Powered Photoelectrochemistry. *Chem. Commun.* **2012**, *48*, 209-211.

(17) Takata, T.; Jiang, J.; Sakata, Y.; Nakabayashi, M.; Shibata, N.; Nandal, V.; Seki, K.; Hisatomi, T.; Domen, K., Photocatalytic Water Splitting with a Quantum Efficiency of Almost Unity. *Nature* **2020**, *581*, 411-414.

(18) Harada, N.; Sasaki, Y.; Hosoyamada, M.; Kimizuka, N.; Yanai, N., Discovery of Key Tips-Naphthalene for Efficient Visible-to-Uv Photon Upconversion under Sunlight and Room Light. *Angew. Chem. Int. Ed.* **2020**, *132*, 1-6.

(19) Yanai, N.; Kozue, M.; Amemori, S.; Kabe, R.; Adachi, C.; Kimizuka, N., Increased Vis-to-Uv Upconversion Performance by Energy Level Matching between a Tadf Donor and High Triplet Energy Acceptors. *J. Mater. Chem. C* **2016**, *4*, 6447-6451.

(20) Duan, P.; Yanai, N.; Kimizuka, N., A Bis-Cyclometalated Iridium Complex as a Benchmark Sensitizer for Efficient Visible-to-Uv Photon Upconversion. *Chem. Commun.* **2014**, *50*, 13111-13113.

(21) Han, J.; Jiang, Y.; Obolda, A.; Duan, P.; Li, F.; Liu, M., Doublet–Triplet Energy Transfer-Dominated Photon Upconversion. *J. Phys. Chem. Lett.* **2017**, *8*, 5865-5870.

(22) Wei, Y.; Xian, H.; Lv, X.; Ni, F.; Cao, X.; Yang, C., Triplet–Triplet Annihilation Upconversion with Reversible Emission-Tunability Induced by Chemical-Stimuli: A Remote Modulator for Photocontrol Isomerization. *Mater. Horizons* **2021**, *8*, 606-611.

(23) Wei, Y.; Li, Y.; Zheng, M.; Zhou, X.; Zou, Y.; Yang, C., Simultaneously High Upconversion Efficiency and Large Anti-Stokes Shift by Using Os (Ii) Complex Dyad as Triplet Photosensitizer. *Adv. Opt. Mater.* **2020**, *8*, 1902157.

(24) Amemori, S.; Sasaki, Y.; Yanai, N.; Kimizuka, N., Near-Infrared-to-Visible Photon Upconversion Sensitized by a Metal Complex with Spin-Forbidden yet Strong S0-T1 Absorption. *J. Am. Chem. Soc.* **2016**, *138*, 8702-8705.

(25) Qi, Y.; Ning, W.; Zou, Y.; Cao, X.; Gong, S.; Yang, C., Peripheral Decoration of Multi-Resonance Molecules as a Versatile Approach for Simultaneous Long-Wavelength and Narrowband Emission. *Adv. Funct. Mater.* **2021**, 10.1002/adfm.202102017.

(26) Peng, J.; Guo, X.; Jiang, X.; Zhao, D.; Ma, Y., Developing Efficient Heavy-Atom-Free Photosensitizers Applicable to Tta Upconversion in Polymer Films. *Chem. Sci.* **2016**, *7*, 1233-1237.

(27) Jiang, X.; Guo, X.; Peng, J.; Zhao, D.; Ma, Y., Triplet-Triplet Annihilation Photon Upconversion in Polymer Thin Film: Sensitizer Design. *ACS Appl. Mater. Interfaces* **2016**, *8*, 11441-11449.

(28) Lee, H.-L.; Lee, M.-S.; Park, H.; Han, W.-S.; Kim, J.-H., Visible-to-Uv Triplet-Triplet Annihilation Upconversion from a Thermally Activated Delayed Fluorescence/Pyrene Pair in

an Air-Saturated Solution. *Korean J. Chem. Eng.* **2019**, *36*, 1791-1798.

(29) Wei, Y.; Zhou, M.; Zhou, Q.; Zhou, X.; Liu, S.; Zhang, S.; Zhang, B., Triplet-Triplet Annihilation Upconversion Kinetics of C60-Bodipy Dyads as Organic Triplet Photosensitizers. *Phys. Chem. Chem. Phys.* **2017**, *19*, 22049-22060.

(30) Wang, Z.; Zhao, J.; Barbon, A.; Toffoletti, A.; Liu, Y.; An, Y.; Xu, L.; Karatay, A.; Yaglioglu, H. G.; Yildiz, E. A., Radical Enhanced Intersystem Crossing (Eisc) in New Bodipy Derivatives and Application for Efficient Triplet-Triplet Annihilation Upconversion. *J. Am. Chem. Soc.* **2017**, *139*, 7831-7842.

(31) Oda, S.; Kumano, W.; Hama, T.; Kawasumi, R.; Yoshiura, K.; Hatakeyama, T., Carbazole-Based Dabna Analogues as Highly Efficient Thermally Activated Delayed Fluorescence Materials for Narrowband Organic Light-Emitting Diodes. *Angew. Chem. Int. Ed.* **2021**, *60*, 2882-2886.

(32) Zhang, Y.; Zhang, D.; Wei, J.; Liu, Z.; Lu, Y.; Duan, L., Multi-Resonance Induced Thermally Activated Delayed Fluorophores for Narrowband Green Oleds. *Angew. Chem. Int. Ed.* **2019**, *58*, 16912-16917.

(33) Kondo, Y.; Yoshiura, K.; Kitera, S.; Nishi, H.; Oda, S.; Gotoh, H.; Sasada, Y.; Yanai, M.; Hatakeyama, T., Narrowband Deep-Blue Organic Light-Emitting Diode Featuring an Organoboron-Based Emitter. *Nat. Photonics* **2019**, *13*, 678-682.

(34) Yang, M.; Park, I. S.; Yasuda, T., Full-Color, Narrowband, and High-Efficiency Electroluminescence from Boron and Carbazole Embedded Polycyclic Heteroaromatics. *J. Am. Chem. Soc.* **2020**, *142*, 19468-19472.

(35) Xu, Y.; Wang, Q.; Cai, X.; Li, C.; Wang, Y., Highly Efficient Electroluminescence from Narrowband Green Circularly Polarized Multiple Resonance Thermally Activated Delayed Fluorescence Enantiomers. *Adv. Mater.* **2021**, *33*, e2100652.

(36) Stavrou, K.; Danos, A.; Hama, T.; Hatakeyama, T.; Monkman, A., Hot Vibrational States in a High-Performance Multiple Resonance Emitter and the Effect of Excimer Quenching on Organic Light-Emitting Diodes. *ACS Appl. Mater. Interfaces* **2021**, *13*, 8643-8655.

(37) Zhao, J.; Chen, K.; Hou, Y.; Che, Y.; Liu, L.; Jia, D., Recent Progress in Heavy Atom-Free Organic Compounds Showing Unexpected Intersystem Crossing (Isc) Ability. *Org. Biomol. Chem.* **2018**, *16*, 3692-3701.

(38) Wu, K.; Zhang, T.; Wang, Z.; Wang, L.; Zhan, L.; Gong, S.; Zhong, C.; Lu, Z.-H.; Zhang, S.; Yang, C., De Novo Design of Excited-State Intramolecular Proton Transfer Emitters Via a Thermally Activated Delayed Fluorescence Channel. *J. Am. Chem. Soc.* **2018**, *140*, 8877-8886.

(39) Li, L.; Zeng, Y.; Chen, J.; Yu, T.; Hu, R.; Yang, G.; Li, Y., Thermally Activated Delayed Fluorescence Via Triplet Fusion. *J. Phys. Chem. Lett.* **2019**, *10*, 6239-6245.

(40) Chen, W.; Song, F.; Tang, S.; Hong, G.; Wu, Y.; Peng, X., Red-to-Blue Photon up-Conversion with High Efficiency Based on a Tadf Fluorescein Derivative. *Chem. Commun.* **2019**, *55*, 4375-4378.

(41) Wei, Y.; Wang, Y.; Zhou, Q.; Zhang, S.; Zhang, B.; Zhou, X.; Liu, S., Solvent Effects on

Triplet–Triplet Annihilation Upconversion Kinetics of Perylene with a Bodipy-Phenyl-C60 Photosensitizer. *Phys. Chem. Chem. Phys.* **2020**, *22*, 26372-26382.

(42) Isokuortti, J.; Allu, S. R.; Efimov, A.; Vuorimaa-Laukkanen, E.; Tkachenko, N. V.; Vinogradov, S. A.; Laaksonen, T.; Durandin, N. A., Endothermic and Exothermic Energy Transfer Made Equally Efficient for Triplet-Triplet Annihilation Upconversion. *J. Phys. Chem. Lett.* **2019**, 318-324.

(43) Kiseleva, N.; Busko, D.; Richards, B. S.; Filatov, M. A.; Turshatov, A., Determination of Upconversion Quantum Yields Using Charge-Transfer State Fluorescence of Heavy-Atom-Free Sensitizer as a Self-Reference. *J. Phys. Chem. Lett.* **2020**, *11*, 6560-6566.

(44) Monguzzi, A.; Mezyk, J.; Scotognella, F.; Tubino, R.; Meinardi, F., Upconversion-Induced Fluorescence in Multicomponent Systems: Steady-State Excitation Power Threshold. *Phys. Rev. B* **2008**, *78*, 195112.

(45) Cheng, Y. Y.; Fückel, B.; Khoury, T.; Clady, R. G.; Tayebjee, M. J.; Ekins-Daukes, N.; Crossley, M. J.; Schmidt, T. W., Kinetic Analysis of Photochemical Upconversion by Triplet− Triplet Annihilation: Beyond Any Spin Statistical Limit. *J. Phys. Chem. Lett.* **2010**, *1*, 1795-1799.

(46) Haefele, A.; Blumhoff, J.; Khnayzer, R. S.; Castellano, F. N., Getting to the (Square) Root of the Problem: How to Make Noncoherent Pumped Upconversion Linear. *J. Phys. Chem. Lett.* **2012**, *3*, 299-303.

(47) Schmidt, T. W.; Castellano, F. N., Photochemical Upconversion: The Primacy of Kinetics. *J. Phys. Chem. Lett.* **2014**, *5*, 4062-4072.

(48) Han, D.; Yang, X.; Han, J.; Zhou, J.; Jiao, T.; Duan, P., Sequentially Amplified Circularly Polarized Ultraviolet Luminescence for Enantioselective Photopolymerization. *Nat. Commun.* **2020**, *11*, 5659.

(49) Huang, L.; Wu, W.; Li, Y.; Huang, K.; Zeng, L.; Lin, W.; Han, G., Highly Effective near-Infrared Activating Triplet-Triplet Annihilation Upconversion for Photoredox Catalysis. *J. Am. Chem. Soc.* **2020**, *143*, 18460-18470.

(50) Ravetz, B. D.; Pun, A. B.; Churchill, E. M.; Congreve, D. N.; Rovis, T.; Campos, L. M., Photoredox Catalysis Using Infrared Light Via Triplet Fusion Upconversion. *Nature* **2019**, *565*, 343-346.

(51) Croisant, M.; Bretz, S. L.; Konkolewicz, D., Investigating Radical Reactivity and Structure–Property Relationships through Photopolymerization. *J. Chem. Educ.* **2019**, *96*, 348-353.

(52) Feist, F.; Rodrigues, L. L.; Walden, S. L.; Krappitz, T. W.; Dargaville, T. R.; Weil, T.; Goldmann, A. S.; Blinco, J. P.; Barner-Kowollik, C., Light-Induced Ligation of O-Quinodimethanes with Gated Fluorescence Self-Reporting. *J. Am. Chem. Soc.* **2020**, *142*, 7744-7748.

(53) Xu, Y.; Li, C.; Li, Z.; Wang, Q.; Cai, X.; Wei, J.; Wang, Y., Constructing Charge-Transfer Excited States Based on Frontier Molecular Orbital Engineering: Narrowband Green Electroluminescence with High Color Purity and Efficiency. *Angew. Chem. Int. Ed.* **2020**, *59*, 17442-17446.

(54) Corrigan, N.; Yeow, J.; Judzewitsch, P.; Xu, J.; Boyer, C., Seeing the Light: Advancing

Materials Chemistry through Photopolymerization. *Angew. Chem. Int. Ed.* **2019**, *58*, 5170-5189.

(55) Dietlin, C.; Schweizer, S.; Xiao, P.; Zhang, J.; Morlet-Savary, F.; Graff, B.; Fouassier, J.-P.; Lalevée, J., Photopolymerization Upon Leds: New Photoinitiating Systems and Strategies. *Polym. Chem.* **2015**, *6*, 3895-3912.

(56) Bagheri, A.; Jin, J., Photopolymerization in 3d Printing. *ACS Appl. Polym. Mater.* **2019**, *1*, 593-611.

(57) Tuten, B. T.; Wiedbrauk, S.; Barner-Kowollik, C., Contemporary Catalyst-Free Photochemistry in Synthetic Macromolecular Science. *Prog. Polym. Sci.* **2020**, *100*, 101183.